Actin chromobody imaging reveals sub-organellar actin dynamics

Cara Schiavon[1*], Tong Zhang[1*], Bing Zhao[2], Leonardo Andrade[1], Melissa Wu[1], Tsung-Chang Sung[3], Yelena Dayn[3], Jasmine W. Feng[4], Omar A. Quintero[4], Robert Grosse[3], Uri Manor[1§]

1. Waitt Advanced Biophotonics Center, Salk Institute for Biological Studies, USA
2. Institute of Experimental and Clinical Pharmacology and Toxicology, University of Freiburg, Germany
3. Transgenic Core, Salk Institute for Biological Studies, USA
4. Department of Biology, University of Richmond, USA

*Contributed equally
§Corresponding author: umanor@salk.edu

Abstract

The actin cytoskeleton plays multiple critical roles in cells, from cell migration to organelle dynamics. The small and transient actin structures regulating organelle dynamics are difficult to detect with fluorescence microscopy. We generated fluorescent protein-tagged actin nanobodies targeted to organelle membranes to enable live cell imaging of sub-organellar actin dynamics with high spatiotemporal resolution. These probes reveal ER-associated actin drives fission of multiple organelles including mitochondria, endosomes, lysosomes, peroxisomes, and the Golgi.

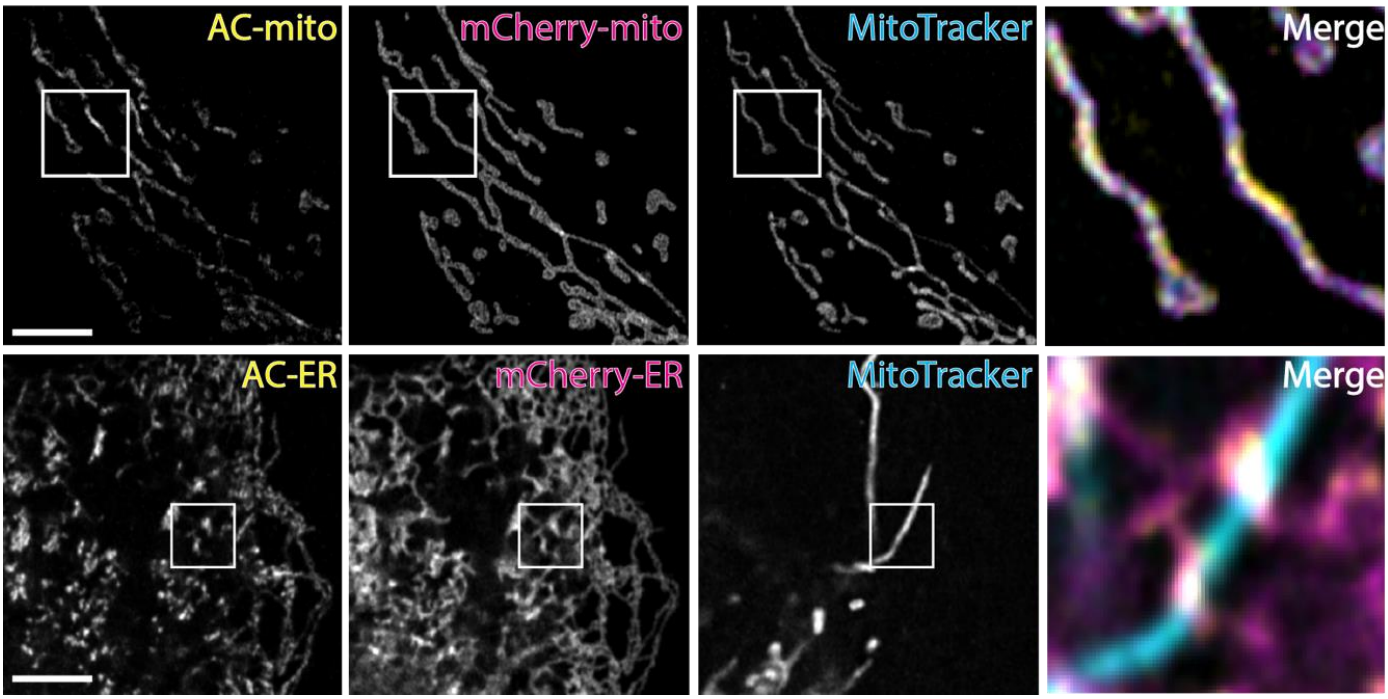

Introduction

The critical role of the actin cytoskeleton in organelle dynamics is largely accepted, but poorly understood. The precise spatiotemporal dynamics of actin at organelle membranes remain particularly unclear due to the combined limitations of currently available actin probes and imaging approaches. For fluorescence microscopy approaches, imaging smaller actin structures in the cell suffers from an enormous background signal issue - the high signal from the dense meshwork of actin filaments throughout the cell overwhelms the signal from the relatively small, transient actin structures associated with organelle dynamics. Furthermore, the limitations in resolution make it difficult to determine whether any actin filaments are physically associated with the organelle. Meanwhile, EM approaches can be used to visualize actin filaments with extremely high resolution[1,2]. However, these techniques only capture single timepoints, making it difficult to determine the precise state or dynamics of the actin filaments or their associated organelles at the time of fixation. All these limitations ultimately preclude a solid understanding of the mechanisms by which actin regulates organelle dynamics in health or disease. Here we employ fluorescent protein-tagged actin nanobodies, aka "actin chromobodies" (AC)[3,4], fused to organelle membrane targeting sequences to facilitate live cell imaging of sub-organellar actin dynamics with high spatiotemporal resolution. Using these probes we discovered that ER-associated actin accumulates at all ER-organelle contacts during organelle fission.

Results

We hypothesized that AC probes with organelle membrane targeting sequences could be used to monitor actin dynamics exclusively within a ~10nm distance from the target organelle membrane. To test this hypothesis, we used the yeast Fis1 mitochondrial outer membrane and Cytb5ER endoplasmic reticulum (ER) minimal C-terminus tail membrane targeting sequences fused to the cytoplasm-facing actin nanobody and tagGFP ("AC-mito" and "AC-ER")[5]. Live cell Airyscan imaging of Hap1 or U2OS cells expressing AC-mito counterstained with MitoTracker dye revealed strikingly specific regions of AC-mito enrichment on the surfaces of mitochondria (Figure 1 and Supplementary Movies 1-2). Similarly, AC-ER expressing cells revealed significant accumulation of AC-ER at specific ER-mitochondria contact sites (Figure 1 and Supplementary Movies 3-4). Interestingly, the AC-ER probe often revealed significant actin accumulation at ER-mitochondria contacts (Figure 1a).

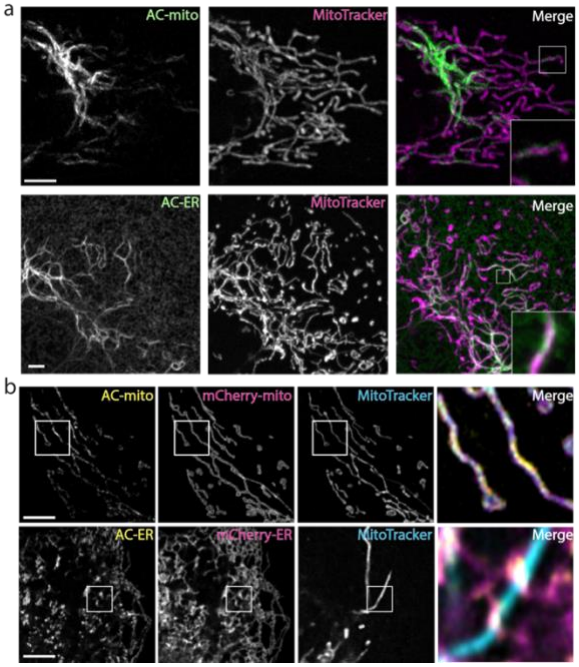

Figure 1|Mitochondria and ER localized actin nanobodies reveal sub-organellar accumulation of actin filaments. a, Hap1 cells expressing actin chromobodies fused to mitochondrial or ER transmembrane domains (AC-mito or AC-ER) reveal localized actin accumulation on mitochondria and the ER, with enhanced accumulation at ER-mitochondria contact sites. **b**, Co-expression of mCherry-mito or mCherry-ER in U2OS cells demonstrates AC-mito and AC-ER accumulation depends on actin nanobody activity. Scale bars: 5 µm.

To rule out the possibility that the membrane targeting sequences we used were causing the probe to accumulate in specific regions independent of actin-binding activity, we generated and co-transfected AC-mito or AC-ER with mCherry-tagged versions of the mitochondrial (Fis1) and ER (Cytb5ER) membrane targeting sequences (mCherry-mito and mCherry-ER). As expected, the mCherry-mito and mCherry-ER signals were evenly distributed along their respective organelle membranes, with no obvious enrichment in any specific regions. In contrast, the co-expressed AC-mito and AC-ER constructs were uniquely enriched in specific regions on their respective organelles (Figure 1b). mCherry-ER showed some accumulation at ER-mitochondria intersections, indicative of stable contacts at these sites[6]. However, the AC-ER probe showed particularly enhanced enrichment at ER-mitochondria contacts, revealing significant accumulation of actin specifically at these contact sites (Figure 1b). These probes thus facilitate unprecedented resolution (10nm from the membrane) and signal-to-background imaging of mitochondria- and ER-associated actin filaments in live cells, validating previous reports and models that actin accumulates at ER-mitochondria intersections, presumably to drive mitochondrial fission[1,7-11]. It should be noted that most (but not all – see Moore et al.[12]) previous live imaging of actin and mitochondria was performed during overexpression or stress conditions in order to increase mitochondrial fission and/or the associated actin signal at mitochondria[7-11,13], whereas these data were obtained under normal physiological conditions.

We considered it important to determine whether the Fis1 membrane targeting sequence in our AC-mito probe might induce dominant negative effects on mitochondrial dynamics by outcompeting endogenous Fis1 for mitochondrial outer membrane localization. Since the AC-mito construct uses only the C-terminal membrane targeting domain of Fis1, an anti-Fis1 antibody against the cytoplasmic N-terminal domain should only detect endogenous protein. We found no change in endogenous Fis1 localization to mitochondria in AC-mito expressing cells compared to neighboring non-transfected cells (Supplementary Figure 1). Finally, to determine whether our localization results were specific to the Fis1 membrane targeting sequence or to actin nanobodies in particular, we generated variants of our AC-mito probe using a different membrane targeting sequence (Cytb5mito[5]) and/or a different F-actin probe (LifeAct[14]). All four of our probes yielded very similar results, revealing specific sub-mitochondrial regions of actin accumulation (Supplementary Figure 2). However, the LifeAct probes displayed a more diffuse localization on the mitochondrial outer membrane. In contrast, our AC probe seemed to better highlight specific subdomains of actin enrichment, consistent with previous comparative studies suggesting that actin nanobodies have superior F-actin labeling capabilities[4]. Thus, we decided to mainly use our AC probes for the majority of our experiments. To further test whether AC-mito accumulation on mitochondria is dependent on F-actin, we treated AC-mito expressing cells with the F-actin depolymerizing drug Latrunculin B (LatB), which significantly reduced the AC-mito signal. Most of the remaining signal appeared as punctate structures, matching the punctate F-actin structures observed with the pan-actin probe AC-tagRFP ("pan-AC") (Supplementary Figure 3). Similar results were observed after treatment with cytochalasin D (Supplementary Movie 5). Taken together, these results strongly support the conclusion that our AC probes are labeling F-actin on their respective membrane surfaces.

In our hands, pan-actin probes such as phalloidin fail to clearly reveal sites of actin accumulation on mitochondria or the ER under normal conditions (Supplementary Figure 4). Furthermore, given the abundance of actin signal throughout the cell and the limitations of resolution in fluorescence microscopy, it is extremely difficult to assess whether colocalization of a pan-actin signal and an organelle membrane is a true actin-membrane association or not. Since our AC probes are small proteins tethered to their respective organelle membranes, we can conclude that all observed actin accumulation is within a maximum distance of 10nm from the organelle membrane (although the distal ends of associated actin filaments may extend far beyond 10nm). Since phalloidin is widely considered the gold standard for F-actin labeling[4], we attempted to colocalize AC-mito and AC-ER with phalloidin staining in fixed cells (Supplementary Figure 5). Interestingly, we found that fixation with 4% PFA causes a dramatic loss in AC-mito enrichment as well as an overall decrease in AC-mito or AC-ER signal, perhaps reflective of the relatively small and transient nature of these membrane-associated actin structures. However, we were still able to detect some co-accumulation of our probes with phalloidin in fixed cells by adjusting the image contrast. Notably, the contrast in the phalloidin signal needed to be extremely high in order to visualize the signal at AC enriched sites (Supplementary Figure 5), causing neighboring structures to be completely saturated or clipped. These results highlight both the value of live imaging labeling approaches as well as why similar actin enriched sites were not previously detected with phalloidin staining. Indeed, only with the AC signal serving as a guide could confidently identify sub-organellar regions of actin enrichment in our phalloidin signal.

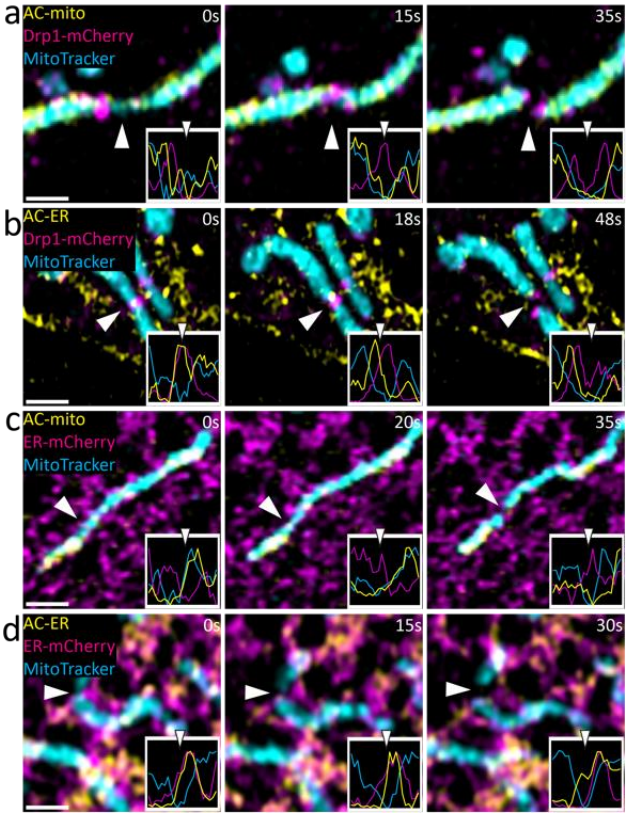

Figure 2|Mitochondria- and ER-associated actin accumulates during mitochondria fission. a, AC-mito accumulates at mitochondrial fission sites prior to Drp1. **b,** AC-ER co-accumulates with Drp1 during mitochondrial fission. **c,** AC-mito accumulates at ER-mediated mitochondrial fission sites. **d,** AC-ER accumulates at ER-tubules driving mitochondrial fission. Scale bars: 1 μm.

Previous studies have demonstrated a role for actin at ER-mitochondria contact sites in driving mitochondrial fission[1,7-11,13,15]. However, due to the abundance of actin in the cytoplasm, it is

difficult to detect actin accumulating near ER-mitochondria contact sites, or whether any such actin directly associates with either organelle using live imaging. To determine whether mitochondria- or ER-associated actin accumulates during ER-mediated fission, we performed live imaging of cells co-expressing AC-mito and mCherry-tagged Drp1, an actin-binding dynamin-related GTPase protein essential for mitochondrial fission[8,16,17] (Figure 2, Supplementary Figure 6, and Supplementary Movies 6-9). To avoid potential overexpression artifacts, we used the low expression ubiquitin promoter C to drive expression of our AC probes[18]. We found that AC-mito accumulates at or immediately adjacent to mitochondrial fission sites prior to Drp1-mediated fission (Figure 2a, Supplementary Movie 6). Interestingly, we frequently observed elongated regions of AC-mito enrichment crossing over mitochondrial constriction sites, consistent with recent reports of similar actin structures observed with platinum replica electron microscopy of membrane extracted cells[1]. We similarly observed accumulation of AC-ER at mitochondrial fission sites prior to Drp1-mediated fission (Figure 2b, Supplementary Movie 7). Co-expression of AC-mito or AC-ER with mCherry-ER showed that both mitochondria- and ER-associated actin accumulates at ER-tubules driving mitochondrial fission (Figure 2c-d, Supplementary Movies 8-9). These results identify a subpopulation of actin filaments specifically associated with the mitochondrial outer membrane and the ER prior to and during ER- and Drp1-mediated mitochondrial fission.

Recent studies have suggested an analogous role for the ER and actin in mediating endosomal fission[19,20]. However, direct evidence is missing. Using our AC-ER probe, we observed actin enrichment at ER-associated endosomal fission sites (Figure 3b, Supplementary Movies 10-11). Given the ER regularly contacts most organelles in the cell more than 90% of the time[21], we hypothesized that actin accumulates at all ER-organelle contact sites to drive their fission. Live imaging of cells co-expressing AC-ER and markers for mitochondria, endosomes, peroxisomes, lysosomes, and the Golgi all revealed accumulation of ER-associated actin at fission sites for each of these organelles (Figure 3a-e, Supplementary Movies 10-14). Scanning electron microscopy (SEM) imaging of cells treated with saponin and cytoskeleton stabilizing buffer shows actin filaments associated with mitochondria in similar patterns observed with AC-mito (Figure 3f). Finally, AC-ER reveals a striking network of ER-associated actin bundles on the nucleus (Figure 3g, Supplementary Movie 15). SEM imaging of non-transfected cells treated with saponin and cytoskeleton stabilizing buffer, we observed a similar network of actin fibers accumulating on the nucleus, validating the localization pattern observed in our AC-ER fluorescence data (Figure 3g). A perinuclear actin cap structure has been previously reported and is known to have important roles in multiple cellular processes[22-27]. However, as with other actin structures, the actin filaments specifically associated with the nucleus have been difficult to visualize with pan-actin probes due to the overwhelming signal from surrounding actin stress fibers and cortical actin. Our data show that AC-ER labeling may provide a more specific labelling approach for visualisation of perinuclear actin cap structures.

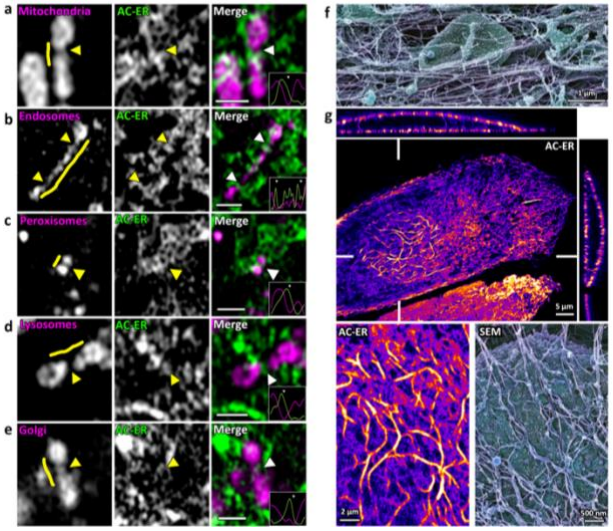

Figure 3|ER-associated actin accumulates at most organelle fission sites. AC-ER accumulates at fission sites in (**a)** mitochondria; **(b)** endosomes (labeled with Rab5a-mCherry); (**c)** peroxisomes (labeled with dsRed-Skl); **(d)** lysosomes (labeled with LAMP1-mCherry); and **(e)** Golgi (labeled with SiT-mApple). **(f)** SEM imaging of actin filament accumulation on a mitochondria. **(g)** AC-ER reveals a distinct pattern of ER-associated actin accumulation around the nucleus. SEM imaging reveals similar structures. Scale bars for a-e: 1 µm

Conclusion

Taken together, our data reveal a novel role for the ER in recruiting actin filaments to all ER-organelle membrane contact sites, most likely in order to drive membrane remodeling and scaffolding for dynamin-mediated organelle fission. Given the important role of both organelle-organelle contact sites and the actin cytoskeleton in health and disease, the apparent ability of the ER to drive actin accumulation at organelle contacts has broad implications for both cell biology and biomedical research. Finally, the ability to use membrane-anchored AC probes as “proximity sensors” for sub-cellular actin dynamics provides a novel tool for studying the role of actin in a wide range of cell biological processes. The variety of subcellular compartments, protein targets, and corresponding subcellular or sub-organellar processes that can be studied with such probes will increase as additional nanobodies and targeting sequences are developed.

Methods

Cell culture. U2OS and Hap1 cells were purchased from ATCC. Cells were grown in DMEM supplemented with 10% fetal bovine serum at 37°C with 5% CO_2. Cells were transfected with Lipofectamine 2000 (ThermoFisher). Cells were plated onto either 8-well #1.5 imaging chambers or #1.5 35mm dishes (Cellvis) that were coated with 10μg/mL fibronectin in PBS at 37°C for 30 minutes prior to plating. 50nM MitoTracker Deep Red (ThermoFisher) was added for 30 minutes then washed for at least 30 minutes to allow for recovery time before imaging in FluoroBrite (ThermoFisher) media.

Airyscan confocal imaging. Cells were imaged with a 63x 1.4NA oil objective on a ZEISS 880 LSM Airyscan confocal system with an inverted stage and heated incubation system with 5% CO_2 control. The GFP channels were imaged with a 488nm laser line at ~500nW laser power. The mCherry or tagRFP channels were imaged with 561nm laser at ~1μW laser power. The MitoTracker Deep Red channel was imaged with ~250nW laser power. For timelapse imaging, the zoom factor was set between 3x-6x to increase the frame rate. In all cases, the maximum pixel dwell time (~0.684μs/pixel) and 2x Nyquist optimal pixel size (~40nm/pixel) was used.

Antibodies. We used the rabbit anti-Fis1 antibody against the N-terminus cytoplasmic facing side of the human Fis1 protein, made by Prestige Antibodies Powered by Atlas Antibodies (Sigma-Aldrich, catalog #: HPA017430). The amino acid sequence of the antigen is MEAVLNELVSVEDLLKFEKKFQSEKAAGSVSKSTQFEYAWCLVRSKYNDDIRKGIVLLEELLPKGS KEEQRDYVFYLAVGNYRLKEYEKALKYVRGLLQTEPQNNQAKELERLIDKAMKKD.

Immunofluorescence. Cells were washed in PBS then fixed with 4% PFA for 30 minutes before permeabilization with 0.1% Triton X-100 for 30 minutes. Cells were then blocked overnight with 4% BSA at 4°C. Cells were then incubated with primary antibody for 2 hours, rinsed 3x with PBS for 10 minutes each, then incubated with secondary antibodies (Jackson Immunoresearch Laboratories) for 1 hour, rinsed 3x with PBS for 10 minutes each, then counterstained with Alexa405-phalloidin (ThermoFisher) for 30 minutes, then rinsed with PBS 3x for 10 minutes each, then mounted with ProLong Glass antifade reagent (ThermoFisher).

Scanning Electron Microscopy. Cells were briefly washed with 0.1 M phosphate-buffered saline (PBS) (37oC) to remove culture media and immediately treated with a membrane extraction solution containing 1% Triton X-100, 100 mM PIPES (pH 7.2), 1 mM EGTA, 1 mM MgCl2, 4.2 % sucrose, 10 μM taxol (Thermo-Scientific) and 10 μM phalloidin (Sigma) for 10 min with gentle rocking at room temperature. Then the samples were washed twice for 5 min in PBS and fixed with 2% glutaraldehyde, 2% paraformaldehyde (Electron Microscopy Sciences - EMS), in 0.1 M sodium cacodylate buffer for 30 min at RT. Samples were washed in the same buffer, post-fixed with 1% OsO4 (EMS) and 1% tannic acid (EMS) for 1h each, dehydrated with a graded ethanol series until absolute and critical point-dried (Leica CPD 030). The samples were coated with a thin platinum layer (4 nm) (Leica EM SCD500) and imaged on a Zeiss Sigma-VP scanning electron microscope at 5 kV.

Image processing and analysis. After acquisition, images were Airyscan processed using the auto-filter 2D-SR settings in Zen Blue (ZEISS). All images were post-processed and analyzed using Imaris (BITPLANE) and Fiji software[28].

Plasmids. Drp1-mCherry was a kind gift from Gia Voeltz (Addgene plasmid #49152). mCherry-Cytob_5RR was a gift from Nica Borgese[29]. EGFP-LifeAct was a gift from Jennifer Rohn [30]. Lamp1-mCherry, SiT-mApple, Sec61-mCherry, and dsRed-Skl were all generous gifts from the Lippincott-Schwartz lab. Rab5a-mCherry was a generous gift from the Merrifield lab (Addgene plasmid #27679). All custom actin nanobody probes were generated starting from the commercial vector of actin chromobody-tagGFP or actin chromobody-tagRFP (ChromoTek) and cloned via the BglII and NotI restriction sites. The following amino acid sequences were attached to the C-terminal of the actin chromobody probes to target the protein either to mitochondria or the ER:

Fis1 (AC-mito and LifeAct-GFP-Fis1):
IQKETLKGVVVAGGVLAGAVAVASFFLRNKRR[5]
Cytb5mito (aka "Cytob_5RR") (AC-GFP-Cytb5mito and LifeAct-GFP-Cytb5mito):
FEPSETLITTVESNSSWWTNWVIPAISALVVALMYRR[31]
Cytb5ER (AC-ER):

IDSSSSWWTNWVIPAISAVAVALMYRLYMAED[5]

LifeAct-GFP-Fis1, LifeAct-GFP-Cytb5mito, and AC-GFP-Cytb5mito were generated using PFU Ultra II for megaprimer PCR insertion[32]. The PCR primers, intended modifications, insert templates, and destination plasmids are listed in Supplemental Table 1 below. All constructs were sequenced completely across their coding region.

Supplemental Table 1: Primers and plasmids used to generate the expression constructs for these studies

Insert plasmid	Destination plasmid	Modification to Destination plasmid	Final Plasmid	Primer Sequence
pAC-tagGFP	pAC-tagGFP-Fis1p	Fis1p localization signal was inserted at the C-terminus of tagGFP via 4 rounds of overlapping PCR, G and P were used as a linker in between Fis1 and GFP	AC-mito (CMV)	fwd: GCGCGCAGATCTAATGGCTCAGGTGCAGCTGGTGGA; rev: ATATAT AGCGGCCGCCTAGCGGCGTTTGTTGCGCAGAAAAAAGCTCGCCACCGCCACCGCGCCCGCCAGCACGCCGCCCGCCACCACCACGCCTTTCAGGGTTTCTTTCTGAATCGGCCCCCTGTACAGCTCGTC
pmCherry	mCherry-Fis1p	Fis1p localization signal was inserted at the C-terminus of mCherry via 4 rounds of overlapping PCR, G and P were used as a linker in between Fis1 and mCherry	mCherry-mito	fwd: GCGCGCAGATCTCCGATGGTGAGCAAGGGCGAGGAG; rev: ATATATAGCGGCCGCCTAGCGGCGTTTGTTGCGCAGAAAAAAGCTCGCCACCGCCACCGCGCCCGCCAGCACGCCGCCCGCCACCACCACGCCTTTCAGGGTTTCTTTCTGAATCGGCCCCCTGTACAGCTCGTC
pAC-tagGFP	AC-ER	Cytb5ER localization signal was inserted at the C-terminus of tagGFP via 4 rounds of overlapping PCR, G and P were used as a linker in between Cytb5ER and tagGFP	AC-ER (CMV promoter)	fwd: GCGCGCAGATCTAATGGCTCAGGTGCAGCTGGTGGA; rev: ATATATAGCGGCCGC CTAATCTTCCGCCATATACAGGCGATACATCAGCGCCACCGCCACCGCGCTAATCGCCGGAATCACCCAGTTGGTCCACCAGCTGCTGCTGCTATCAAT CGGCCCCCTGTACAGCTCGTC
mcherry-Cytob_5RR	EGFP-Lifeact	insertion of CytoB5RR sequence at C-terminus of EGFP with GGSGGGGS linker in between	LifeAct-GFP-Cytb5mito	fwd: TCTCGGCATGGACGAGCTGTACAAGGGTGGATCTGGAGGTGGCG rev: GATTATGATCTAGAGTCGCGGCCGCTTATTAACGCCGGTACATCAGCGCTA
pAC-tagGFP-Fis1p	EGFP-Lifeact	insertion of Fis1p sequence at C-terminus of EGFP	LifeAct-GFP-Fis1	fwd: TCTCGGCATGGACGAGCTGTACAAGGGTGGATCTGGAGGTGGCG rev:TCTCGGCATGGACGAGCTGTACAAGGGGCCGATTCAGAAAGAAACCCT
mcherry-Cytob_5RR	AC-mito	replace Fis1p localization signal with CytoB5RR signal with a GGSGGGGS linker in between	AC-GFP-Cytb5mito	fwd: GATTATGATCTAGAGTCGCGGCCGCTTAGCGGCGTTTGTTGCGCAGAAAAAA rev: ACGGCATGGACGAGCTGTACAGGGGTGGATCTGGAGGTGGCG
pLV hUbC-dCas9 VP64-T2A-GFP	pSin-CMV-AC-mito	The UbC promoter region was synthesized from pLV hUbC-dCas9 VP64-T2A-GFPusing Q5 Hot Start High-Fidelity DNA polymerase with additions of the EcoRI (5'end) and NheI (3'end) restriction enzyme sites. The DNA fragment of Ac-TagGFP-Fis1 DNA fragment was taken from pSin-CMV-AC-TagGFP- Fis1 by cutting with NheI and KpnI restriction enzymes. Two DNA fragments were cloned into the pSin lentiviral vector digested with EcoRI and KpnI.	AC-mito (UbC promoter – used in experiments)	fwd: TTAAGGGAATTCGGCCTCCGCGCCG; rev: GCCCAAGCTAGCGTCTAACAAAAAAG CCAAAAACGG.
pLV hUbC-dCas9 VP64-T2A-GFP	pSin-CMV-AC-ER	The UbC promoter region was synthesized from pLV hUbC-dCas9 VP64-T2A-GFP with additions of the EcoRI (5'end) and NheI (3'end) restriction enzyme sites. The DNA fragment of Ac-TagGFP-Cytb5 DNA fragment was taken from pSin-CMV-AC-TagGFP-Cytb5 by cutting with NheI and KpnI restriction enzymes. The two DNA fragments were cloned into the pSin lentiviral vector digested with EcoRI and KpnI.	AC-ER (UbC promoter - used in experiments)	fwd: TTAAGGGAATTCGGCCTCCGCGCCG; rev: GCCCAAGCTAGCGTCTAACAAAAAAG CCAAAAACGG.
pAC-TagGFP-Cytb5	mCherry-mito	pmCherry-Fis1 plasmid was cut with BsrGI and NotI restriction enzymes to remove the Fis1 coding region and replaced with the Cytb5 coding region cut with BsrGI and NotI restriction enzymes from the pAC-TagGFP-Cytb5 plasmid using Quick Ligation Kit.	ER-mCherry	n/a.

Acknowledgements

The Waitt Advanced Biophotonics Center is funded by the Waitt Foundation and Core Grant applications NCI CCSG (CA014195) and NINDS Neuroscience Center (NS072031). This work was supported by the Transgenic Core Facility of the Salk Institute with funding from NIH-NCI CCSG: P30 014195. R.G. laboratory is funded by grants from HFSP RGP0021/2016 and the Cluster of Excellence CIBSS- Centre for Integrative Biological Signalling Studies. O.A.Q. lab is supported by NIGMS Grant R15 GM119077 and by funding from the University of Richmond School of Arts & Sciences.

Figure 1

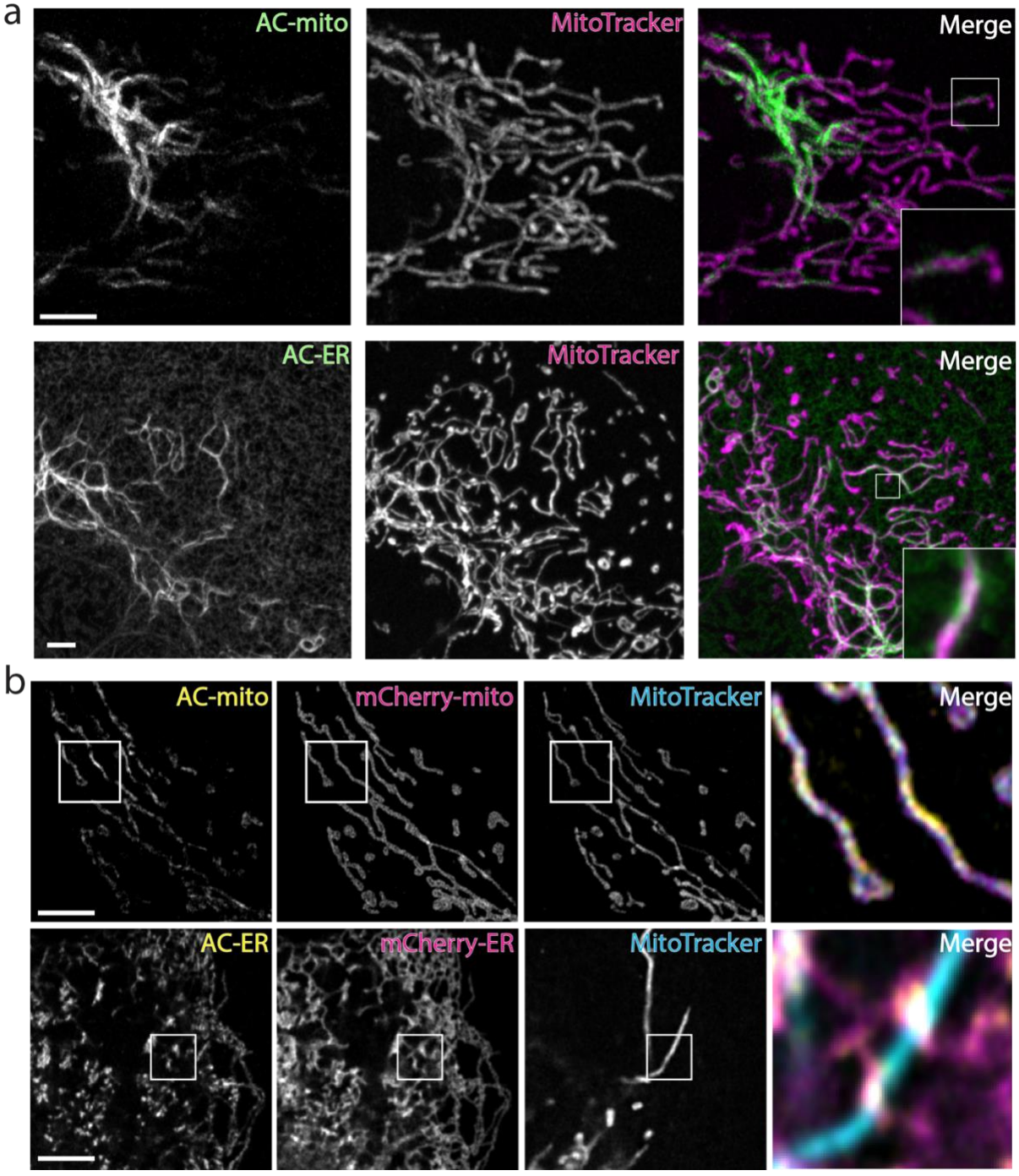

Figure 1|Mitochondria and ER localized actin nanobodies reveal suborganellar accumulation of actin filaments. a, Actin chromobodies fused to the Fis1- or Cytb5ER transmembrane domains (AC-mito or AC-ER) reveal localized actin accumulation on mitochondria and the ER, with enhanced accumulation at ER-mitochondria contact sites. **b**, Co-expression of AC-mito or AC-ER with mCherry-tagged versions lacking nanobody domains reveal accumulation to be specific to actin-binding activity. Scale bars: 5 μm.

Supplementary Figure 1

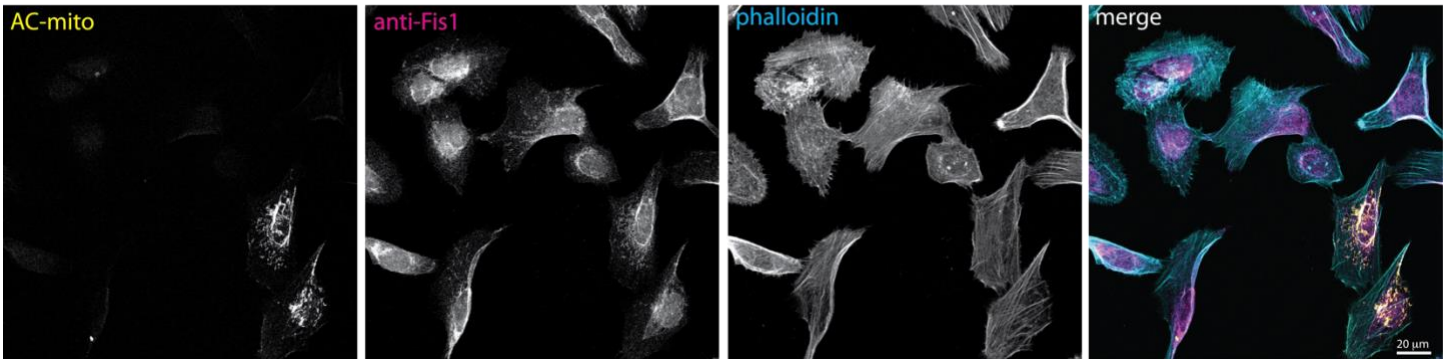

Supplementary Figure 1|AC-mito expression does not alter endogenous Fis1 localization to mitochondria. Cells expressing AC-mito show similar levels of endogenous anti-Fis1 immunofluorescence as non-transfected cells. Note that the anti-Fis1 antigen is not present in the AC-mito protein. Scale bar: 20 µm.

Supplementary Figure 2

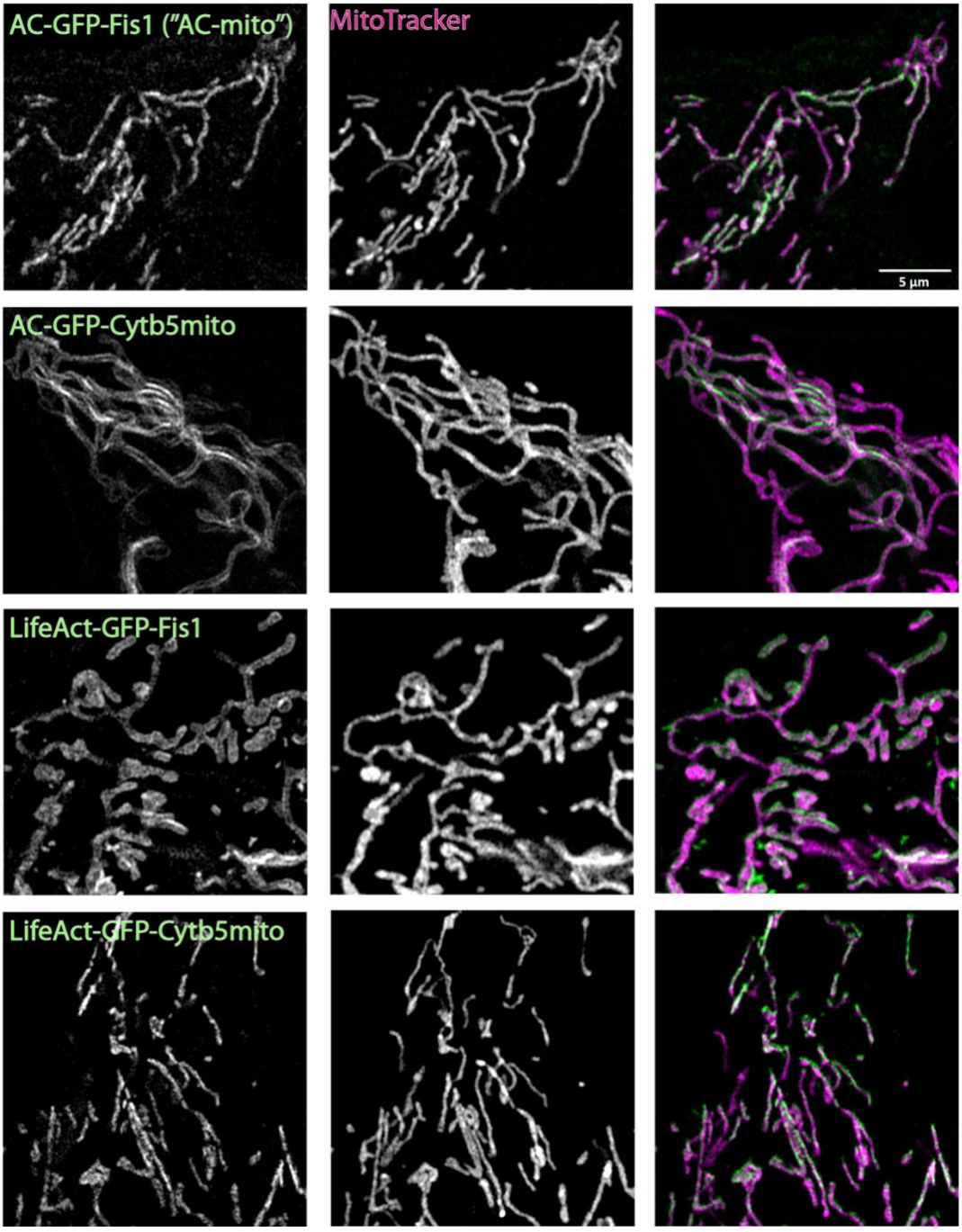

Supplementary Figure 2|Alternate membrane-targeting and actin-binding motifs yield similar results. Switching the Fis1 mitochondrial outer membrane targeting sequence for Cytb5mito (Cytb5mito-AC-GFP) yields similar results. Similarly, switching the actin nanobody motif with LifeAct (Fis1-LifeAct-GFP) also yields similar results. Scale bar: 5 µm.

Supplementary Figure 3

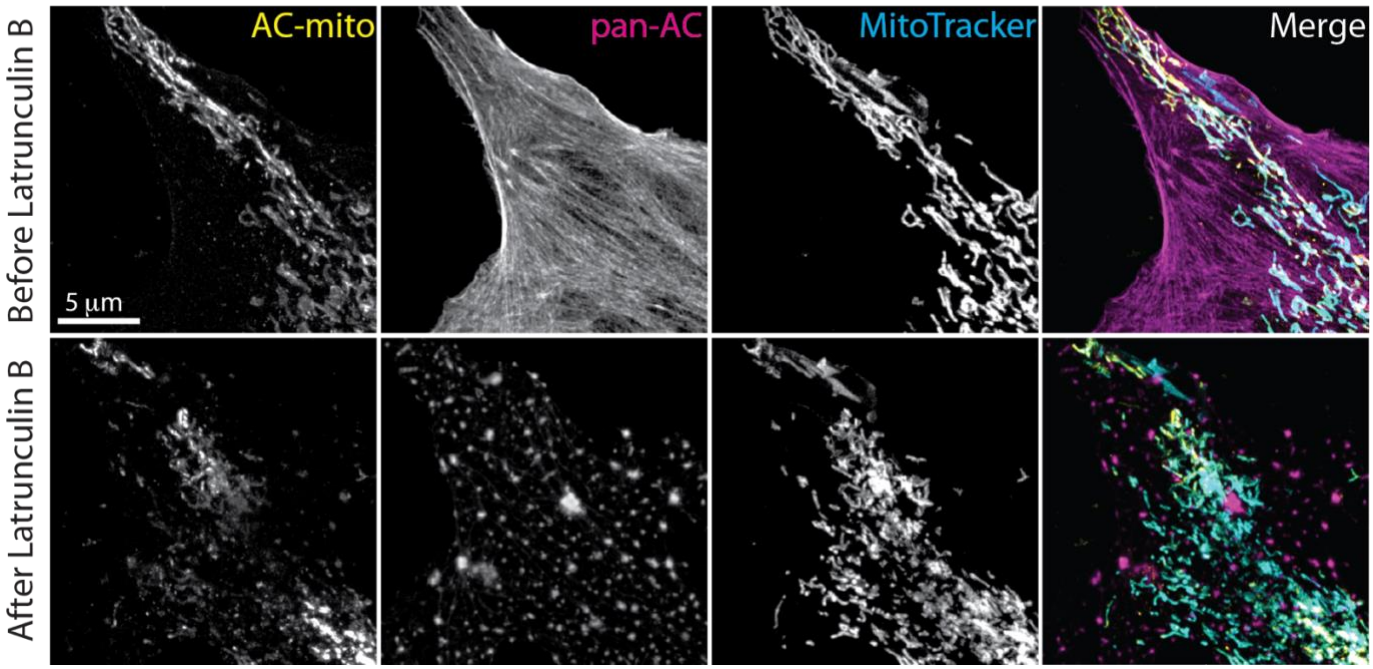

Supplementary Figure 3|Actin depolymerization destroys AC-mito localization. Cells expressing AC-mito and pan-AC, a pan-actin probe (AC-tagRFP), were imaged before and after treatment with Latrunculin B for 30 minutes. After Latrunculin B treatment, AC-mito displayed much less accumulation at specific regions on mitochondria. Scale bar: 5 μm

Supplementary Figure 4

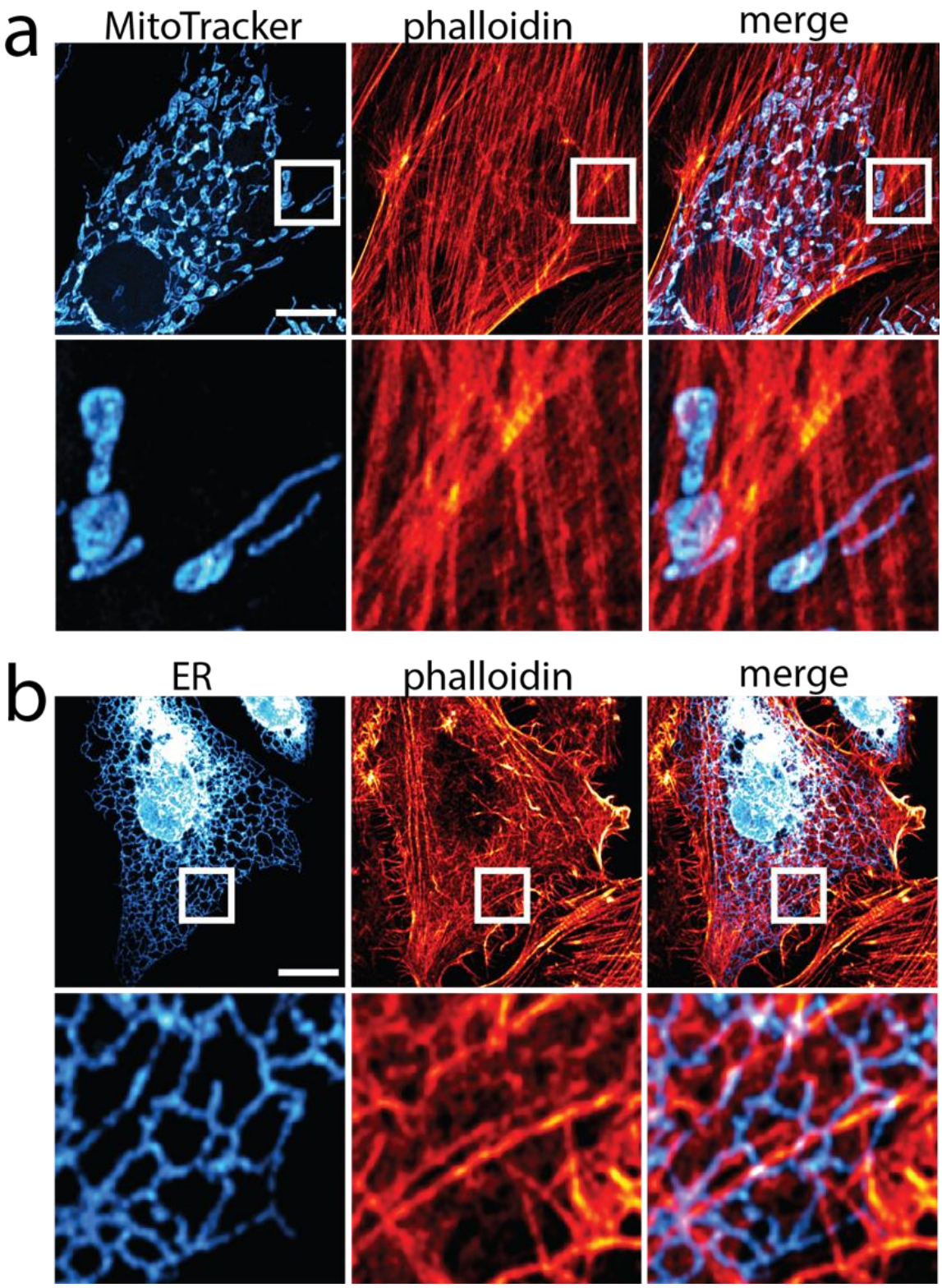

Supplementary Figure 4|Phalloidin staining does not show obvious accumulation of actin on mitochondria or ER. a, Cells stained with phalloidin and MitoTracker do not show obvious accumulation of actin on mitochondria. **b,** Cells expressing the ER marker Sec61-mCherry counterstained with phalloidin do not show obvious accumulation of actin on any specific region of the ER. Scale bar: 10μm.

Supplementary Figure 5

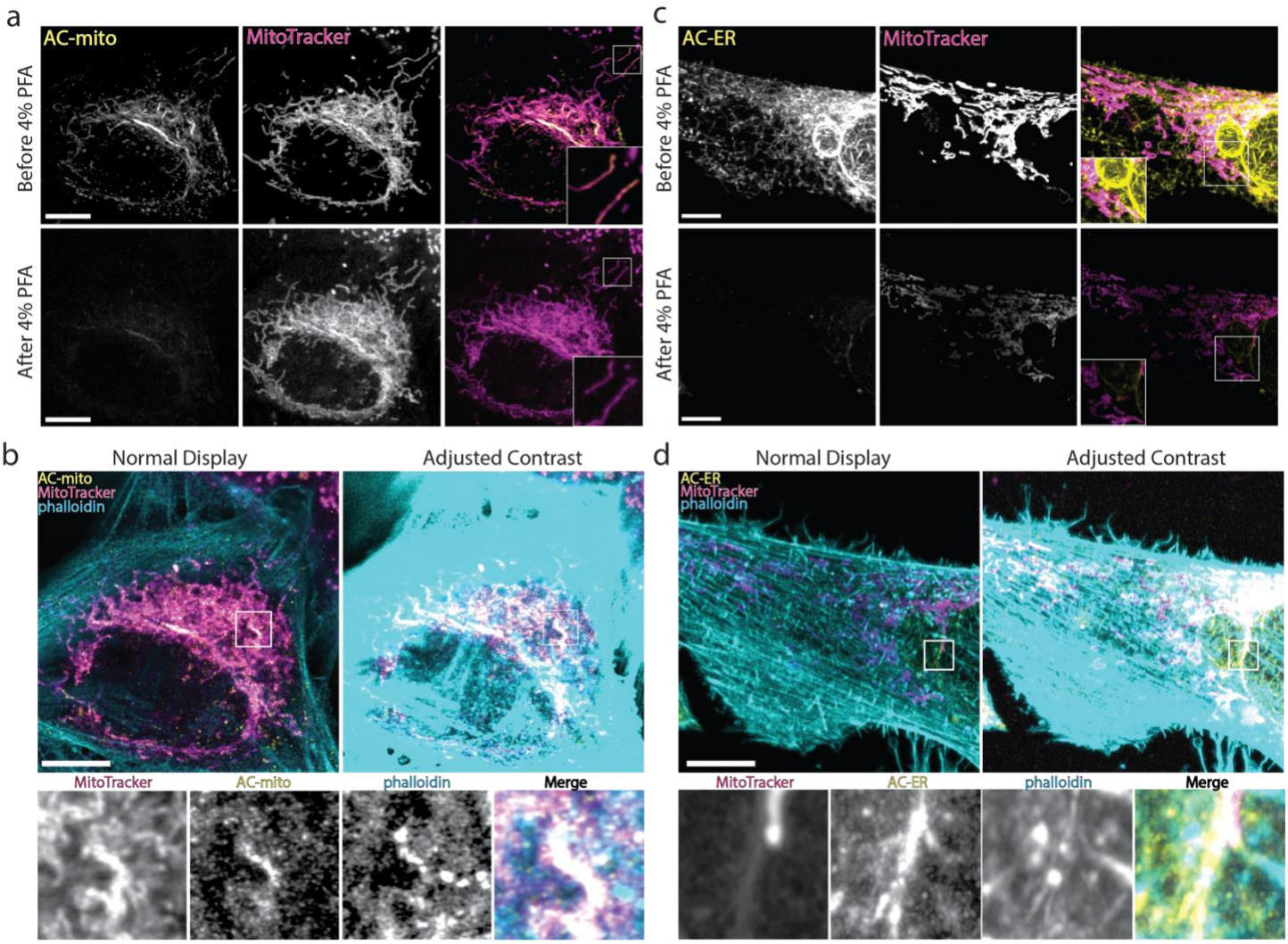

Supplementary Figure 5|Most sub-organellar actin accumulation does not survive conventional fixation. **a+c** Imaging the same cell expressing AC-mito or AC-ER before and 30 minutes after fixation with 4% PFA reveals a significant decrease in AC-mito or AC-ER signal after fixation. **b+d,** phalloidin colocalizes with AC-mito and AC-ER, but with much lower signal than surrounding larger actin structures. Bottom row shows insets with adjusted contrast. Scale bars: 10 μm.

Figure 2

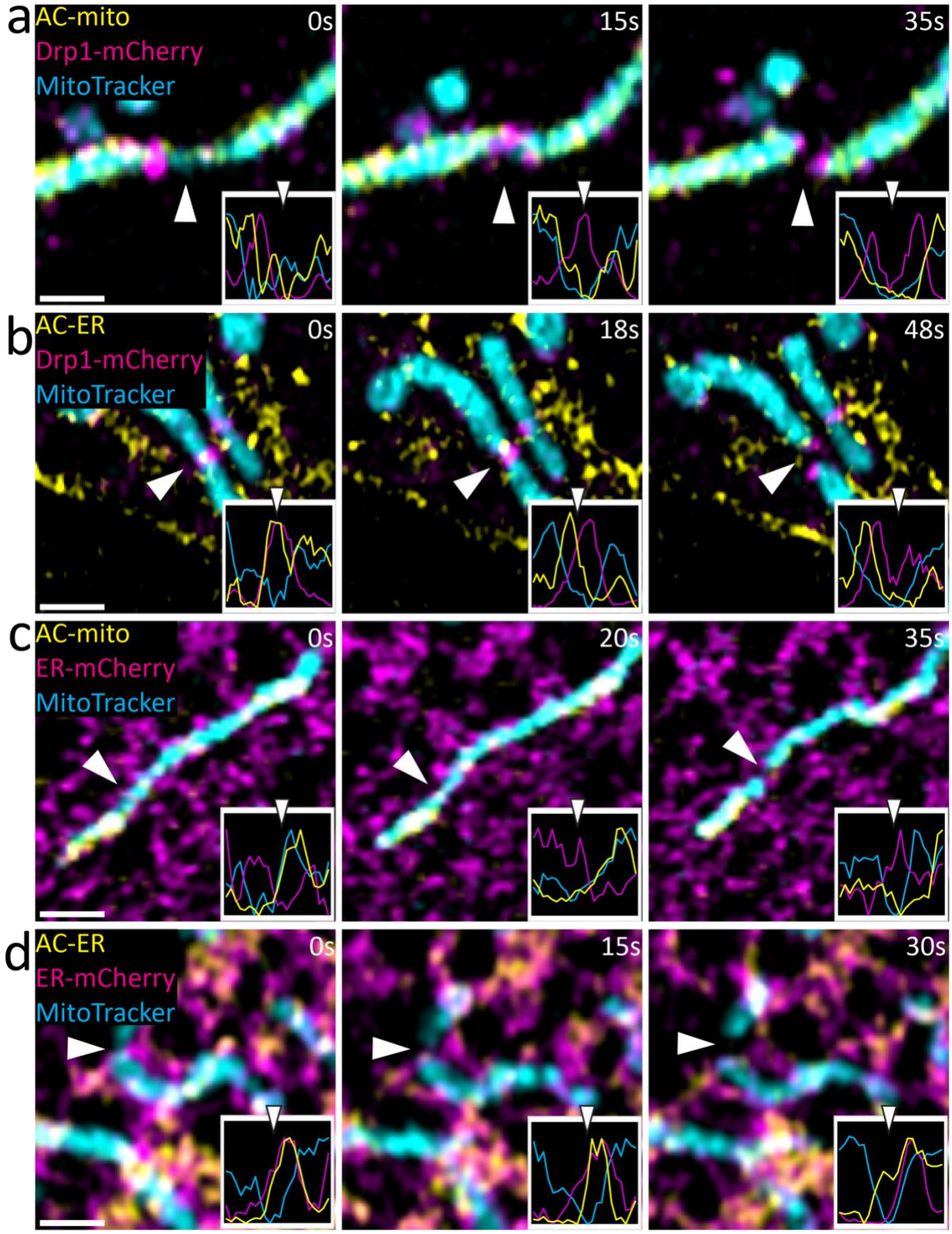

Figure 2|Mitochondria- and ER-associated actin accumulates during mitochondria fission. a, AC-mito accumulates at mitochondrial fission sites prior to Drp1. **b,** AC-ER co-accumulates with Drp1 during mitochondrial fission. **c,** AC-mito accumulates at ER-mediated mitochondrial fission sites. **d,** AC-ER accumulates at ER-tubules driving mitochondrial fission. Scale bars: 1 μm.

Supplementary Figure 6

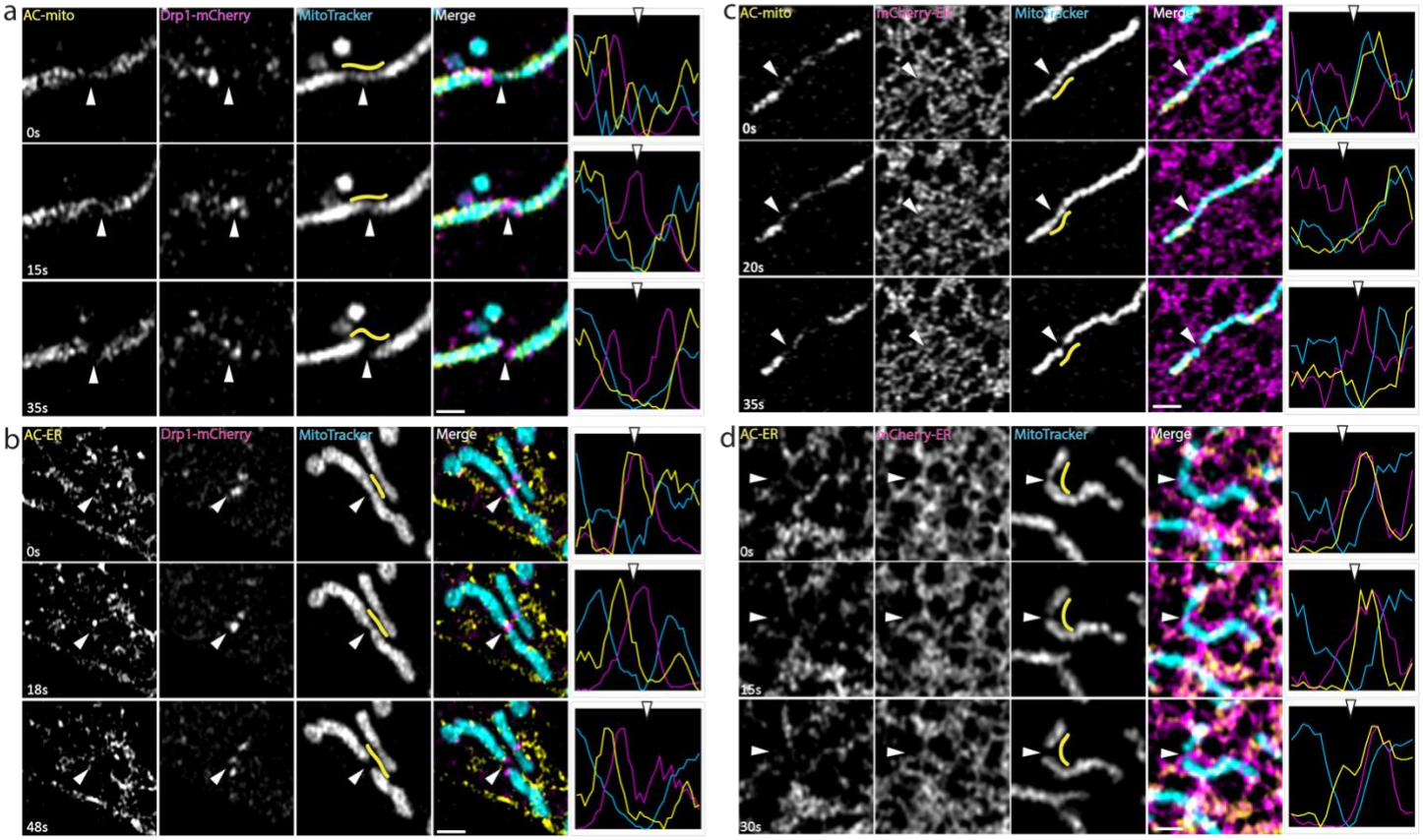

Supplementary Figure 6|Live imaging of AC probes reveal actin accumulation at mitochondrial fission sites. **a,** AC-mito accumulates prior to Drp1 during mitochondrial fission. **b,** AC-ER accumulates at mitochondrial fission sites with Drp1. **c,** AC-mito accumulates at ER-mitochondria contact sites prior to mitochondrial fission. **d,** AC-ER specifically accumulates at ER-mitochondria contact sites prior to mitochondrial fission. Scale bars: 500nm.

Figure 3

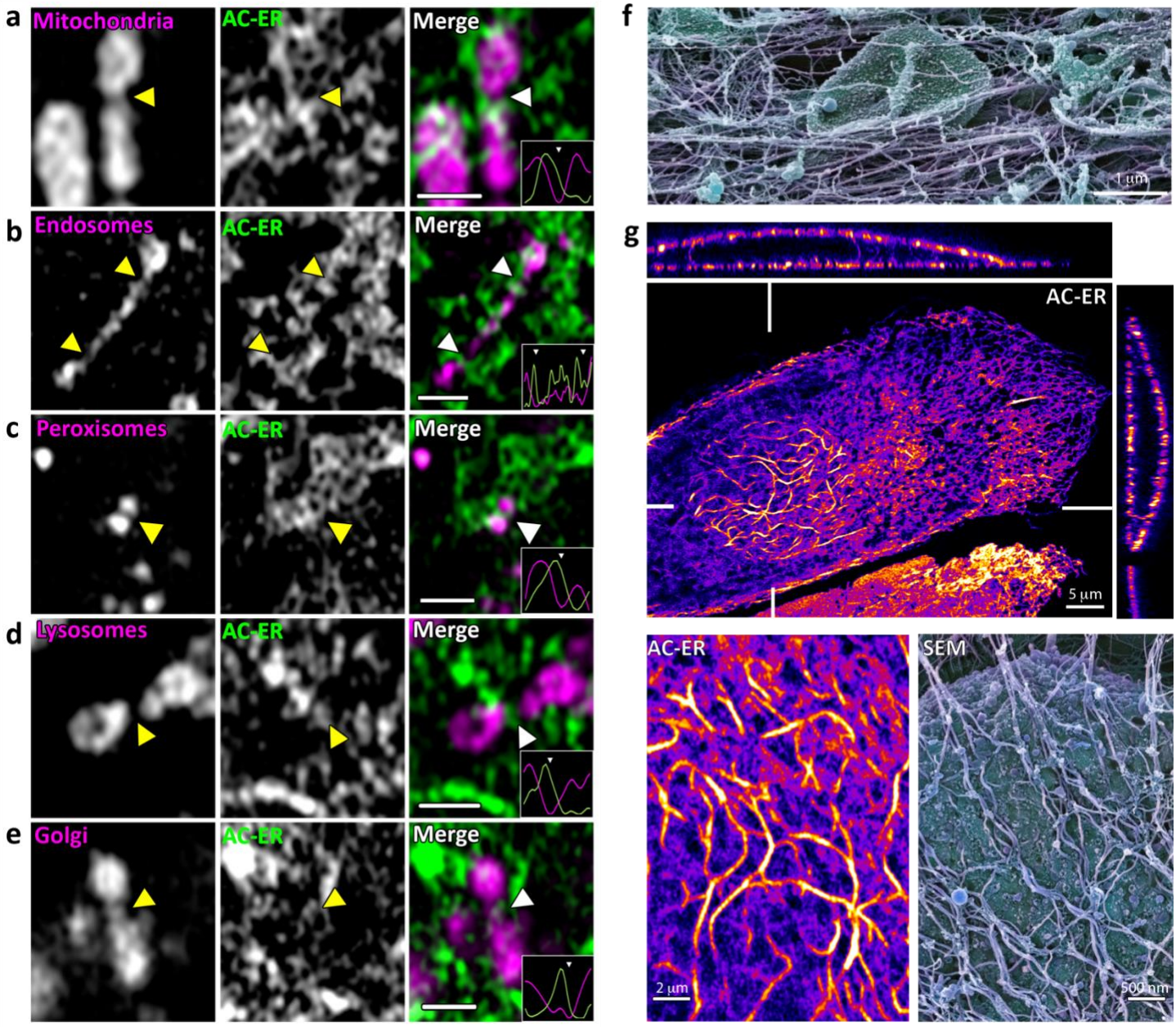

Figure 3|ER-associated actin accumulates at most organelle fission sites. AC-ER accumulates at fission sites in (**a)** mitochondria; **(b)** endosomes (labeled with Rab5a-mCherry); (**c)** peroxisomes (labeled with dsRed-Skl); **(d)** lysosomes (labeled with LAMP1-mCherry); and **(e)** Golgi (labeled with SiT-mApple). **(f)** SEM image of actin filament association with a mitochondrion. **(g)** AC-ER reveals a distinct pattern of ER-associated actin accumulation around the nucleus. SEM imaging of membrane extracted cells reveals similar structures. Scale bars for a-e: 1 µm

Supplementary Movie 1|Live cell imaging of mitochondria-associated actin. A Hap1 cell expressing AC-mito counterstained with MitoTracker shows dynamic subdomains of actin enrichment on mitochondria.

Supplementary Movie 2|Live cell imaging of mitochondria-associated actin. A Hap1 cell expressing AC-mito counterstained with MitoTracker shows dynamic subdomains of actin enrichment on mitochondria (example 2).

Supplementary Movie 3|Live cell imaging of ER-associated actin. A Hap1 cell expressing AC-ER counterstained with MitoTracker shows dynamic subdomains of actin enrichment on the ER, in particular at ER-mitochondria contact sites.

Supplementary Movie 4|Live cell imaging of ER-associated actin. A Hap1 cell expressing AC-ER counterstained with MitoTracker shows dynamic subdomains of actin enrichment on the ER, in particular at ER-mitochondria contact sites (example 2).

Supplementary Movie 5|Live imaging of AC-mito expressing cells before and after Cytochalasin D treatment. Live imaging of Cytochalasin D untreated (left) vs. treated (right) AC-mito expressing U2OS cells.

Supplementary Movie 6|Live imaging of AC-mito and Drp1 during mitochondrial fission. Live imaging of AC-mito and Drp1-mCherry in U2OS cells counterstained with MitoTracker reveals accumulation of mitochondria-associated actin prior to Drp1-mediated fission.

Supplementary Movie 7|Live imaging of AC-ER and Drp1 during mitochondrial fission. Live imaging of AC-ER and Drp1-mCherry in U2OS cells counterstained with MitoTracker reveals accumulation of ER-associated actin prior to Drp1-mediated fission.

Supplementary Movie 8|Live imaging of AC-mito and the ER during mitochondrial fission. Live imaging of AC-mito and mCherry-ER in U2OS cells counterstained with MitoTracker reveals accumulation of mitochondria-associated actin prior to ER-mediated fission.

Supplementary Movie 9|Live imaging of AC-ER and the ER during mitochondrial fission. Live imaging of AC-ER and mCherry-ER in U2OS cells counterstained with MitoTracker reveals accumulation of ER-associated actin prior to ER-mediated fission.

Supplementary Movie 10|ER-associated actin accumulates at mitochondrial fission sites. AC-ER accumulation at a fission site in MitoTracker-labeled mitochondria. Scale bar: 1 µm

Supplementary Movie 11|ER-associated actin accumulates at endosomal fission sites. AC-ER accumulation at two fission sites in Rab5a-mCherry-labeled endosomes. Scale bar: 1 µm

Supplementary Movie 12|ER-associated actin accumulates at peroxisomal fission sites. AC-ER accumulation at a fission site in dsRed-Skl-labeled peroxisomes. Scale bar: 1 µm

Supplementary Movie 13|ER-associated actin accumulates at lysosomal fission sites. AC-ER accumulation at a fission site in LAMP1-mCherry-labeled lysosomes. Scale bar: 1 µm

Supplementary Movie 14|ER-associated actin accumulates at Golgi fission sites. AC-ER accumulation at a fission site in SiT-mApple-labeled Golgi. Scale bar: 1 µm

Supplementary Movie 15|ER-associated actin forms a network on the nucleus. 3D rendering of a U2OS cell expressing AC-ER reveals accumulation around the surface of the nucleus. Cyan: AC-ER. Orange: MitoTracker.

References

1 Yang, C. & Svitkina, T. M. Ultrastructure and dynamics of the actin-myosin II cytoskeleton during mitochondrial fission. *Nat Cell Biol* **21**, 603-613, doi:10.1038/s41556-019-0313-6 (2019).

2 Jasnin, M. *et al.* Three-dimensional architecture of actin filaments in Listeria monocytogenes comet tails. *Proc Natl Acad Sci U S A* **110**, 20521-20526, doi:10.1073/pnas.1320155110 (2013).

3 Rocchetti, A., Hawes, C. & Kriechbaumer, V. Fluorescent labelling of the actin cytoskeleton in plants using a cameloid antibody. *Plant Methods* **10**, 12, doi:10.1186/1746-4811-10-12 (2014).

4 Melak, M., Plessner, M. & Grosse, R. Actin visualization at a glance. *J Cell Sci* **130**, 525-530, doi:10.1242/jcs.189068 (2017).

5 Rapaport, D. Finding the right organelle. Targeting signals in mitochondrial outer-membrane proteins. *EMBO reports* **4**, 948-952, doi:10.1038/sj.embor.embor937 (2003).

6 Friedman, J. R. *et al.* ER tubules mark sites of mitochondrial division. *Science* **334**, 358-362, doi:10.1126/science.1207385 (2011).

7 Manor, U. *et al.* A mitochondria-anchored isoform of the actin-nucleating spire protein regulates mitochondrial division. *eLife* **4**, doi:10.7554/eLife.08828 (2015).

8 Ji, W. K., Hatch, A. L., Merrill, R. A., Strack, S. & Higgs, H. N. Actin filaments target the oligomeric maturation of the dynamin GTPase Drp1 to mitochondrial fission sites. *eLife* **4**, e11553, doi:10.7554/eLife.11553 (2015).

9 Chakrabarti, R. *et al.* INF2-mediated actin polymerization at the ER stimulates mitochondrial calcium uptake, inner membrane constriction, and division. *J Cell Biol* **217**, 251-268, doi:10.1083/jcb.201709111 (2018).

10 Korobova, F., Ramabhadran, V. & Higgs, H. N. An actin-dependent step in mitochondrial fission mediated by the ER-associated formin INF2. *Science* **339**, 464-467, doi:10.1126/science.1228360 (2013).

11 Korobova, F., Gauvin, T. J. & Higgs, H. N. A role for myosin II in mammalian mitochondrial fission. *Curr Biol* **24**, 409-414, doi:10.1016/j.cub.2013.12.032 (2014).

12 Moore, A. S., Wong, Y. C., Simpson, C. L. & Holzbaur, E. L. Dynamic actin cycling through mitochondrial subpopulations locally regulates the fission-fusion balance within mitochondrial networks. *Nature communications* **7**, 12886, doi:10.1038/ncomms12886 (2016).

13 Li, S. *et al.* Transient assembly of F-actin on the outer mitochondrial membrane contributes to mitochondrial fission. *J Cell Biol* **208**, 109-123, doi:10.1083/jcb.201404050 (2015).

14 Riedl, J. *et al.* Lifeact: a versatile marker to visualize F-actin. *Nat Methods* **5**, 605-607, doi:10.1038/nmeth.1220 (2008).

15 De Vos, K. J., Allan, V. J., Grierson, A. J. & Sheetz, M. P. Mitochondrial function and actin regulate dynamin-related protein 1-dependent mitochondrial fission. *Curr Biol* **15**, 678-683, doi:10.1016/j.cub.2005.02.064 (2005).

16 Hatch, A. L., Ji, W. K., Merrill, R. A., Strack, S. & Higgs, H. N. Actin filaments as dynamic reservoirs for Drp1 recruitment. *Mol Biol Cell* **27**, 3109-3121, doi:10.1091/mbc.E16-03-0193 (2016).

17 Smirnova, E., Griparic, L., Shurland, D. L. & van der Bliek, A. M. Dynamin-related protein Drp1 is required for mitochondrial division in mammalian cells. *Mol Biol Cell* **12**, 2245-2256, doi:10.1091/mbc.12.8.2245 (2001).

18 Qin, J. Y. *et al.* Systematic comparison of constitutive promoters and the doxycycline-inducible promoter. *PLoS One* **5**, e10611, doi:10.1371/journal.pone.0010611 (2010).

19 Rowland, A. A., Chitwood, P. J., Phillips, M. J. & Voeltz, G. K. ER contact sites define the position and timing of endosome fission. *Cell* **159**, 1027-1041, doi:10.1016/j.cell.2014.10.023 (2014).

20 Hoyer, M. J. *et al.* A Novel Class of ER Membrane Proteins Regulates ER-Associated Endosome Fission. *Cell* **175**, 254-265 e214, doi:10.1016/j.cell.2018.08.030 (2018).

21 Valm, A. M. *et al.* Applying systems-level spectral imaging and analysis to reveal the organelle interactome. *Nature* **546**, 162-167, doi:10.1038/nature22369 (2017).

22 Gay, O. *et al.* RefilinB (FAM101B) targets filamin A to organize perinuclear actin networks and regulates nuclear shape. *Proc Natl Acad Sci U S A* **108**, 11464-11469, doi:10.1073/pnas.1104211108 (2011).

23 Woroniuk, A. *et al.* STEF/TIAM2-mediated Rac1 activity at the nuclear envelope regulates the perinuclear actin cap. *Nature communications* **9**, 2124, doi:10.1038/s41467-018-04404-4 (2018).

24 Kim, D. H., Cho, S. & Wirtz, D. Tight coupling between nucleus and cell migration through the perinuclear actin cap. *J Cell Sci* **127**, 2528-2541, doi:10.1242/jcs.144345 (2014).

25 Khatau, S. B., Kim, D. H., Hale, C. M., Bloom, R. J. & Wirtz, D. The perinuclear actin cap in health and disease. *Nucleus* **1**, 337-342, doi:10.4161/nucl.1.4.12331 (2010).

26 Khatau, S. B. *et al.* A perinuclear actin cap regulates nuclear shape. *Proc Natl Acad Sci U S A* **106**, 19017-19022, doi:10.1073/pnas.0908686106 (2009).

27 Chambliss, A. B. *et al.* The LINC-anchored actin cap connects the extracellular milieu to the nucleus for ultrafast mechanotransduction. *Sci Rep* **3**, 1087, doi:10.1038/srep01087 (2013).

28 Schindelin, J. *et al.* Fiji: an open-source platform for biological-image analysis. *Nat Methods* **9**, 676-682, doi:10.1038/nmeth.2019 (2012).

29 Borgese, N., Gazzoni, I., Barberi, M., Colombo, S. & Pedrazzini, E. Targeting of a tail-anchored protein to endoplasmic reticulum and mitochondrial outer membrane by independent but competing pathways. *Molecular Biology of the Cell* **12**, 2482-2496 (2001).

30 Rohn, J. L. *et al.* Myo19 ensures symmetric partitioning of mitochondria and coupling of mitochondrial segregation to cell division. *Curr Biol* **24**, 2598-2605, doi:10.1016/j.cub.2014.09.045 (2014).

31 Borgese, N., Gazzoni, I., Barberi, M., Colombo, S. & Pedrazzini, E. Targeting of a tail-anchored protein to endoplasmic reticulum and mitochondrial outer membrane by independent but competing pathways. *Mol Biol Cell* **12**, 2482-2496, doi:10.1091/mbc.12.8.2482 (2001).

32 Geiser, M., Cebe, R., Drewello, D. & Schmitz, R. Integration of PCR fragments at any specific site within cloning vectors without the use of restriction enzymes and DNA ligase. *BioTechniques* **31**, 88-90, 92 (2001).

Figure 1

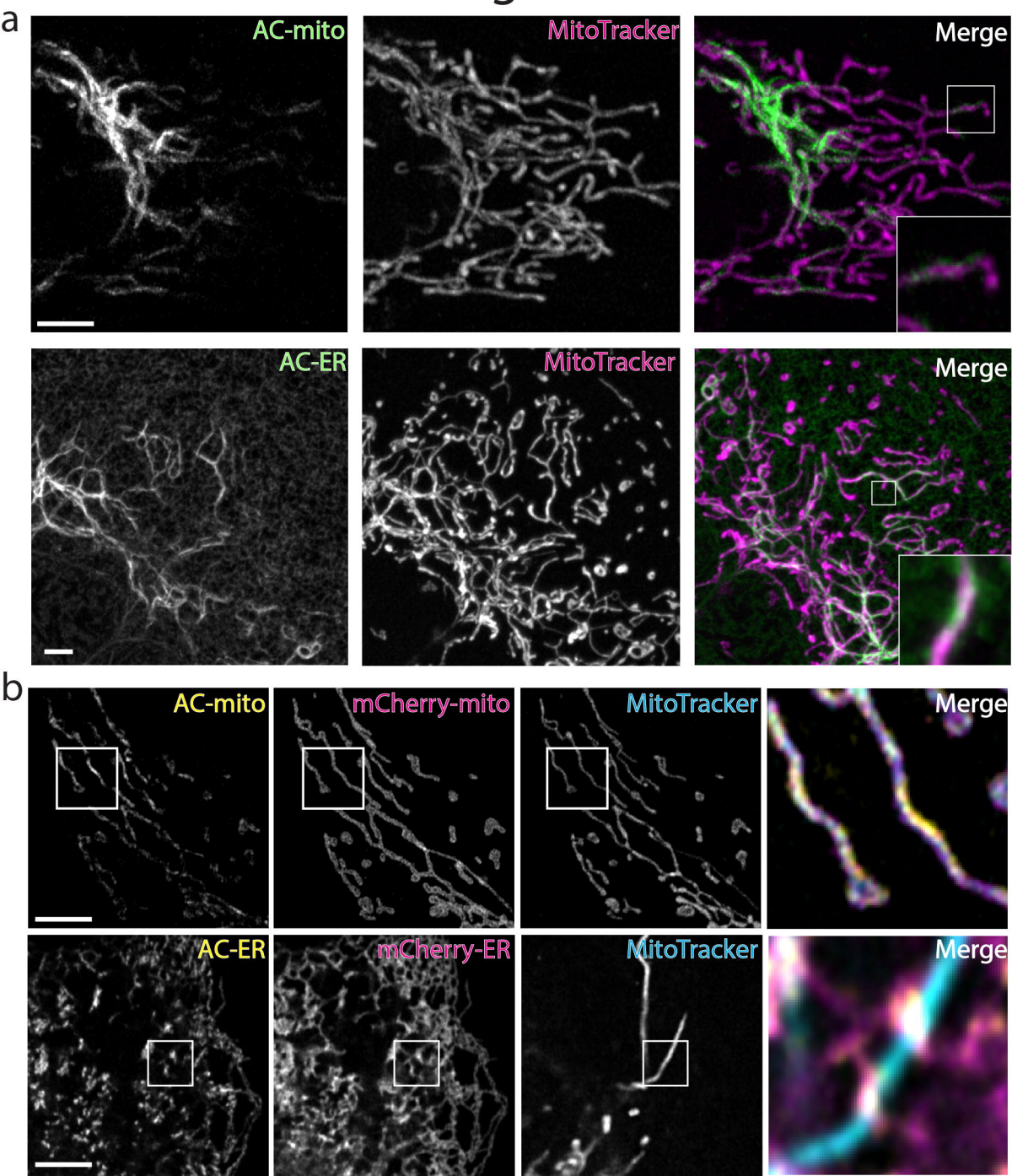
a
AC-mito
MitoTracker
Merge
AC-ER
MitoTracker
Merge
b
AC-mito
mCherry-mito
MitoTracker
Merge
AC-ER
mCherry-ER
MitoTracker
Merge

Figure 2

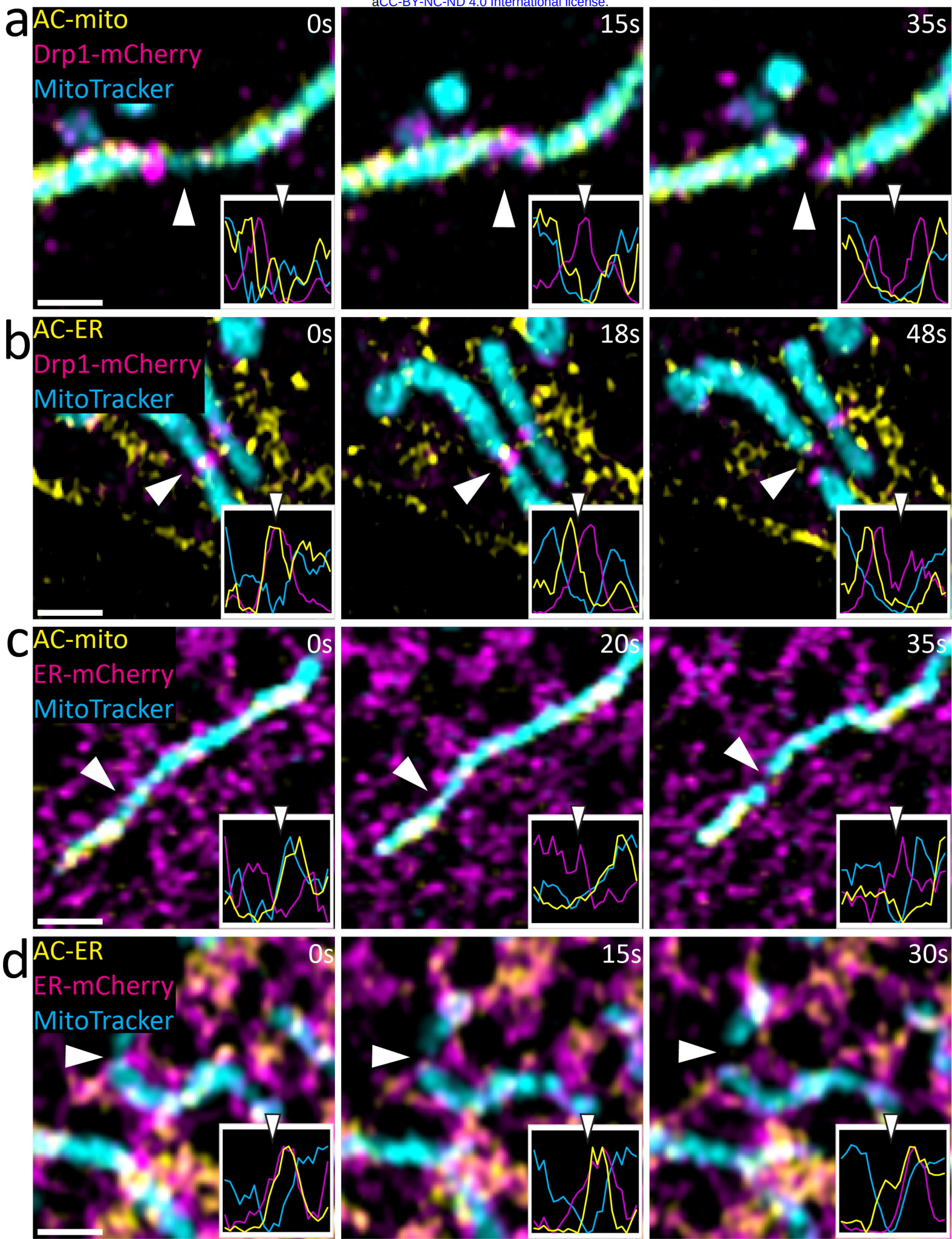

Figure 3

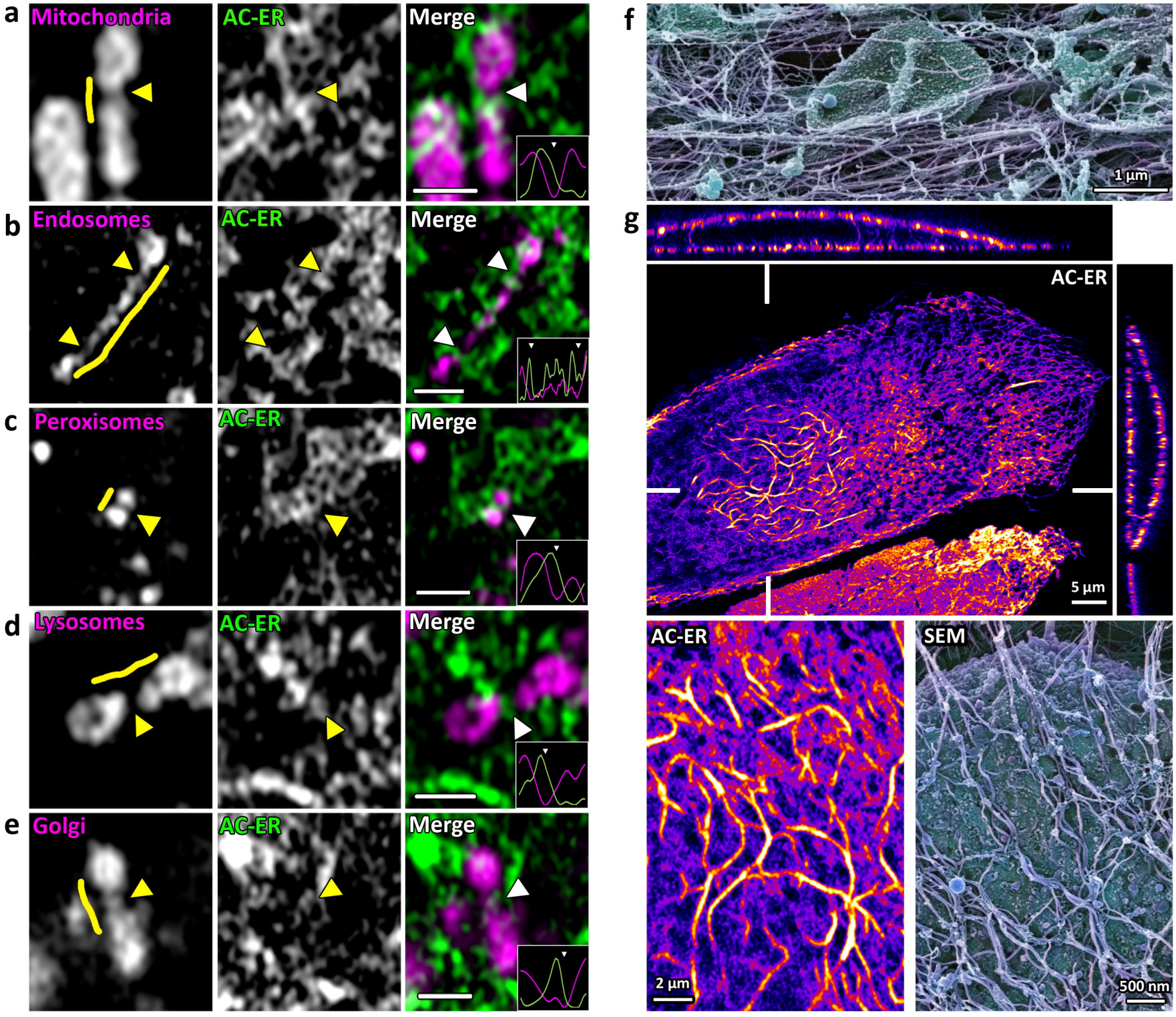
a
Mitochondria
AC-ER
Merge
b
Endosomes
AC-ER
Merge
c
Peroxisomes
AC-ER
Merge
d
Lysosomes
AC-ER
Merge
e
Golgi
AC-ER
Merge
f
1 µm
g
AC-ER
5 µm
AC-ER
2 µm
SEM
500 nm

Supplementary Figure 1

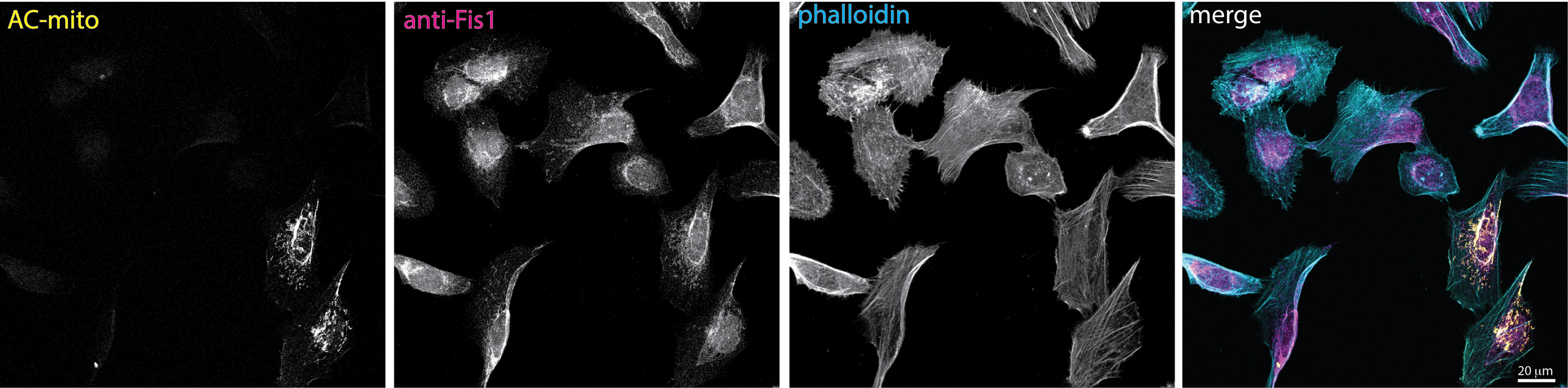

Supplementary Figure 2

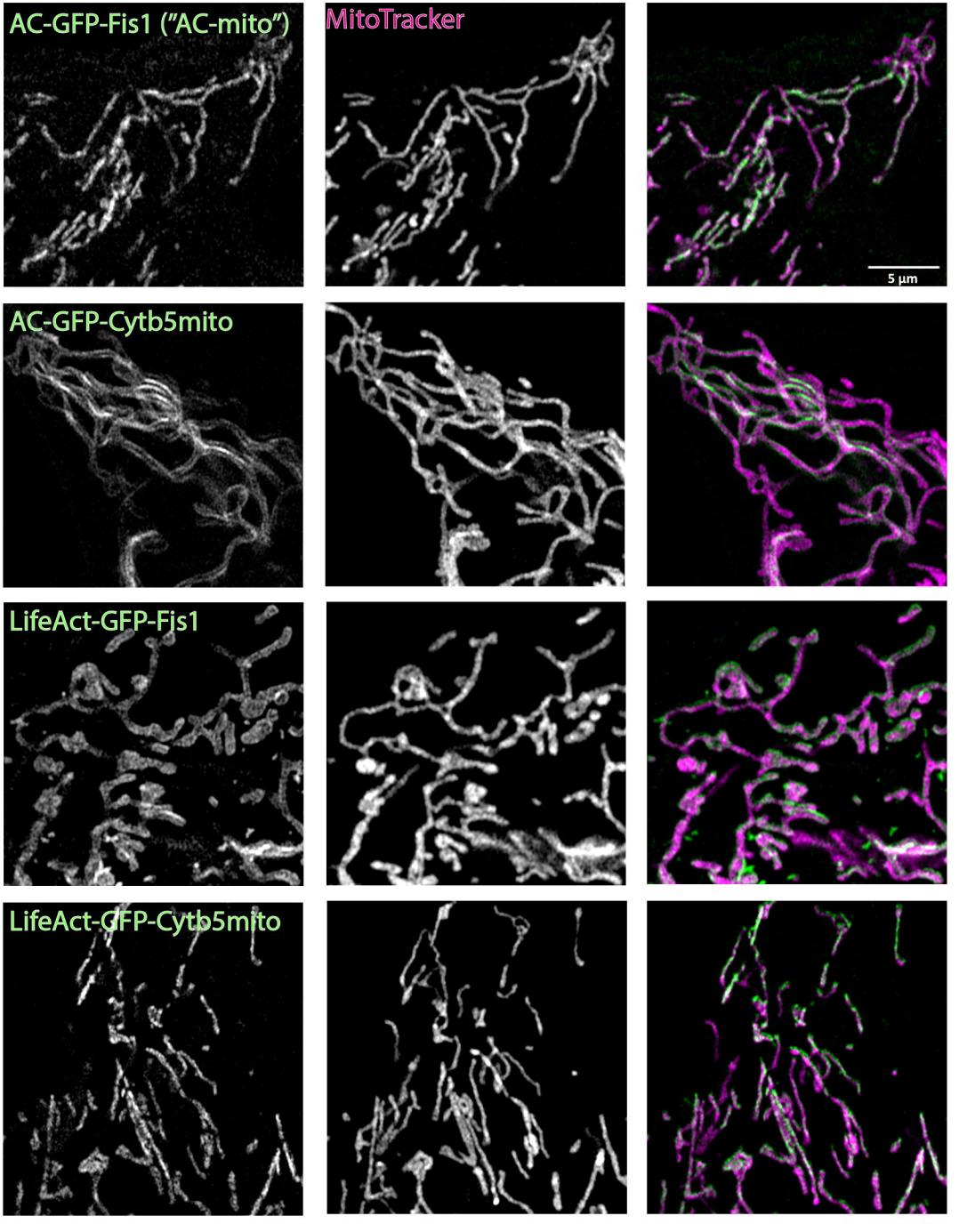

Supplementary Figure 3

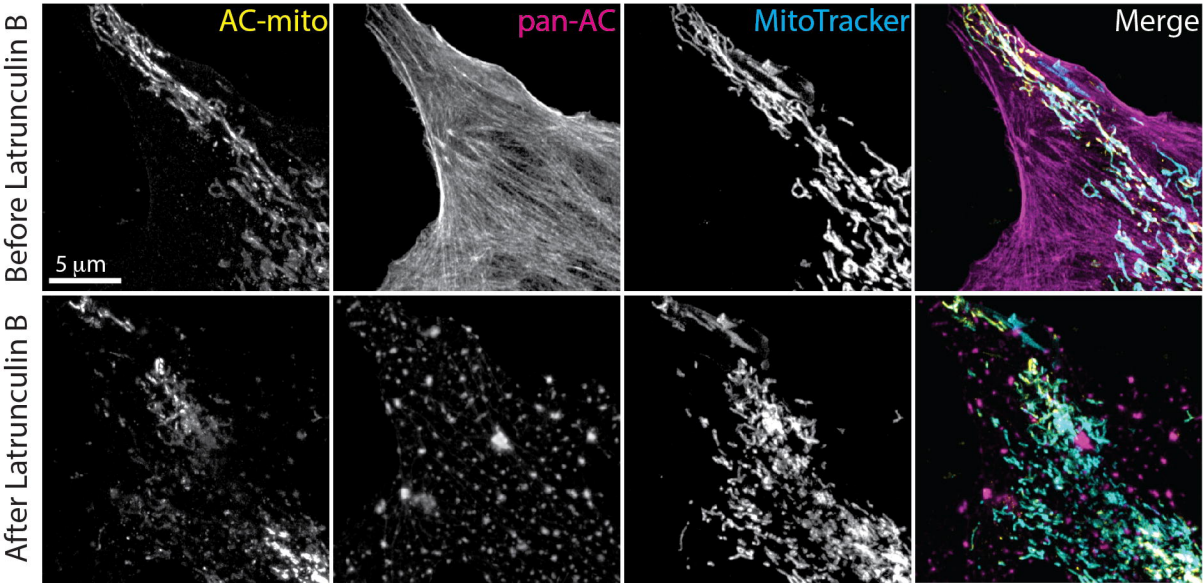

Supplementary Figure 4

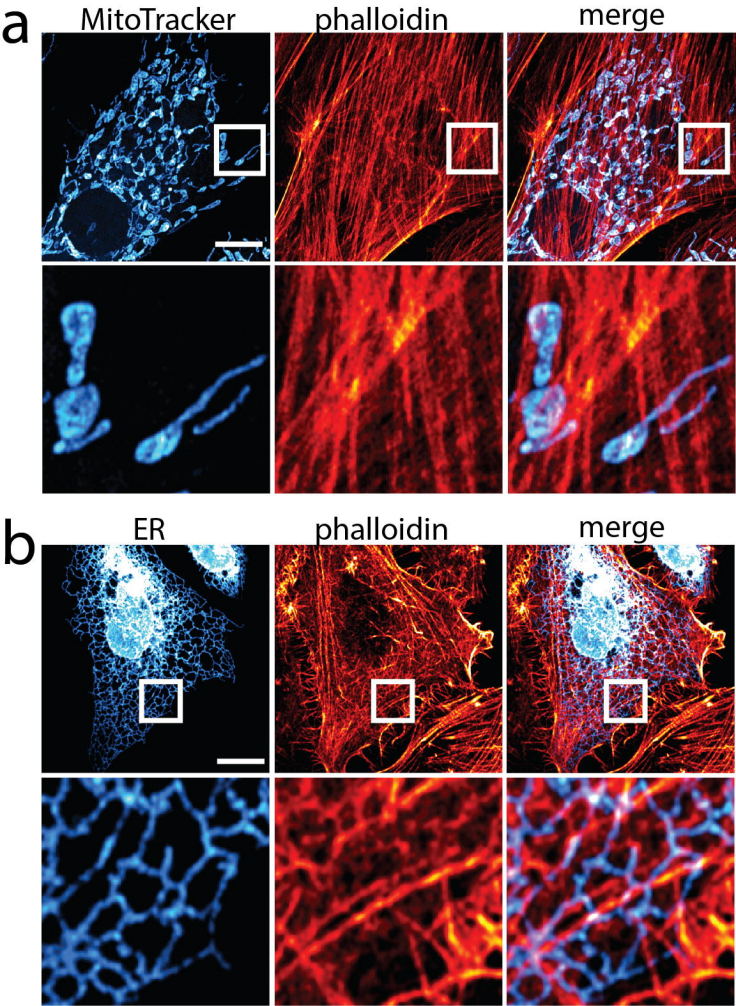

Supplementary Figure 5

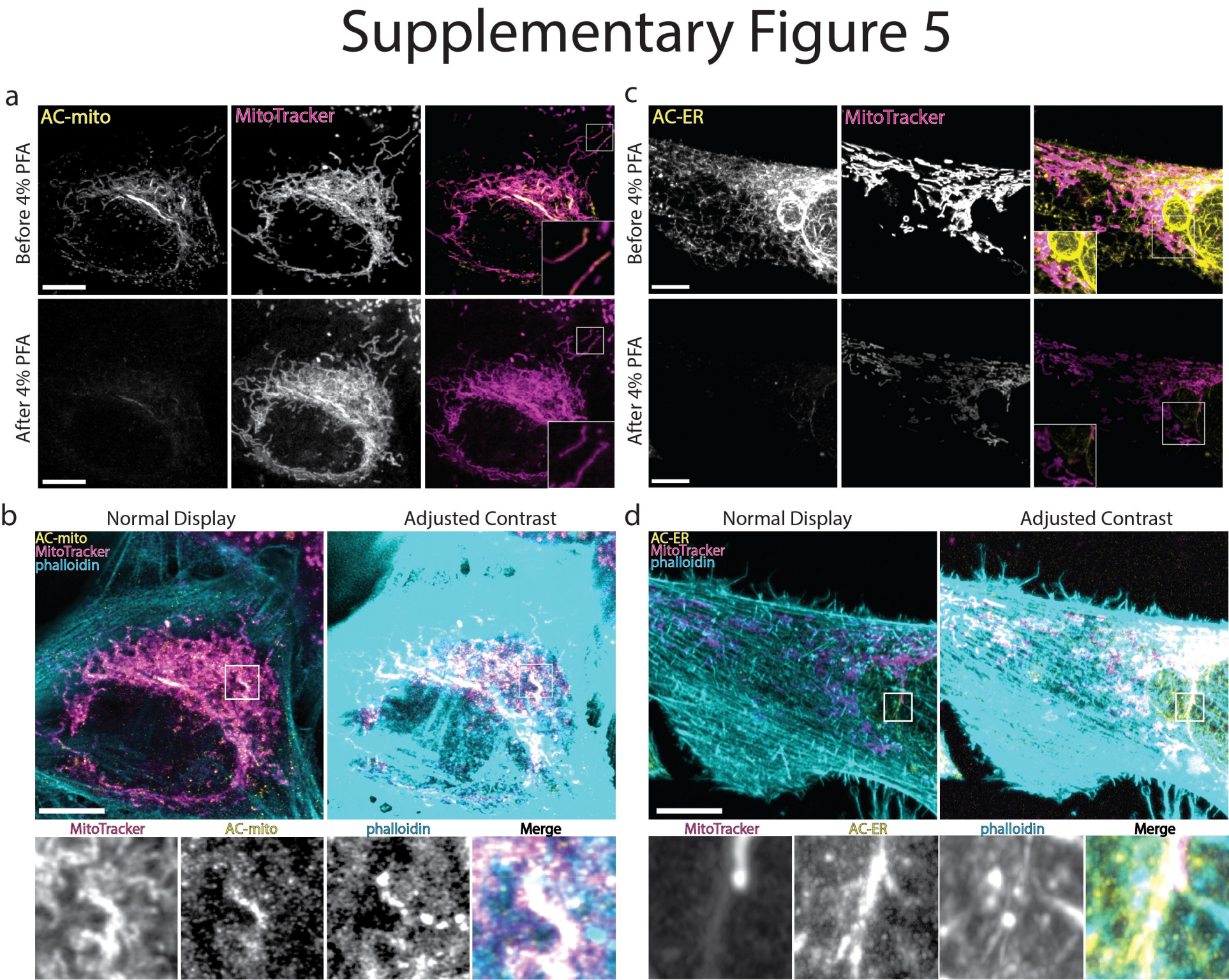

Supplementary Figure 6